Vestnik Otdelenia nauk o Zemle RAN, VOL. 3, NZ6009, doi:10.2205/2011NZ000139, 2011

Origin of the stratification of cratonic mantle lithosphere

I. V. Ashchepkov[1], D. A. Ionov[2], T. Ntaflos[3], H. Downes[4], P.V. Afanasiev[1]
[1]Institute of Geology and mineralogy SB RAS, Novosibirsk
[2]University of Lyone, France
[3]University of Vienna, Austria
[4]University of London, Great Britain

Key words: Mantle, thermobarometry, layering, lithosphere, craton, heat flow

Citation: Ashchepkov, I. V., D. A. Ionov, T. Ntaflos, H. Downes, V. P. Afanasiev (2011), Origin of the stratification of cratonic mantle lithosphere, *Vestn. Otd. nauk Zemle, 3*, NZ6009, doi:10.2205/2011NZ000139.

Compiled PTX diagram and trans-sects for sub-cratonic mantle lithosphere (SCLM) >of 150 kimberlitic pipes including those from Yakutia.

Major regularities were determined for by the comparison of the PTX diagram for the subcratonic lithospheric mantle (SCLM) according to mantle xenoliths from large amount of the kimberlite pipes from N America Yakutia, Baltica , South and Central Africa. Proterozoic pipes from Africa like Premier Roberts Victor show in general higher heating degree which is visible especially by the by the high temperature PT subadiabatic arrays for SCLM beneath Premier from the deep level at 70 kbar (Fig. 1). The diamond inclusions and diamond eclogites from Roberts Victor support this thesis. (Fig 2).

But common pipes beneath Kaapvaal craton refer to 40mw/m2 geotherm in the middle part and heating at 60 kbar and different PT paths for the mantle eclogites. Diamond inclusions reveal colder and deeper conditions and several PT paths.

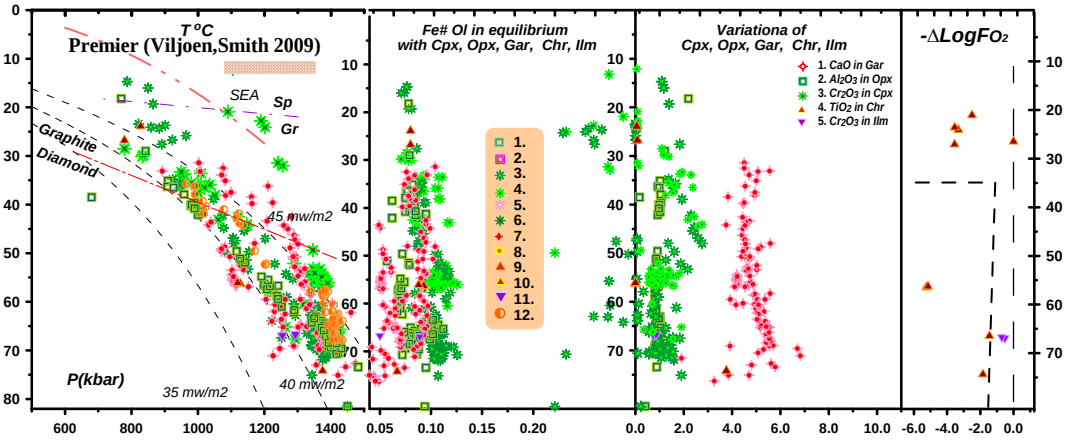

Fig 1. PTXF diagram for the mantle beneath the Proterozoic Premier pipe S Africa. Signs for orthopyroxene: 1. T°C [*Brey and Kohler,* 1990]) -P (kbar) [*McGregor*, 1974]. 2. the same for diamond inclusions; clinopyroxene: 3. T°C [*Nimis and Taylor*, 2000] – P [*Ashchepkov*, 2010]; 4. P and T°C *Nimis, Taylor* , 2000. 5. the same for eclogites; 6. the same fore diamond eclogites. Garnet: 7. T°C [*O'Neil and Wood,* 1979, monomineral]- P [*Ashchepkov et al.*, 2010]. 8. the same for the diamond inclusions; chromite: 9.T°C [*O'Neil and Wall*, 1987], monomineral]- P [kbar] [*Ashchepkov et al.*, 2010]; 10. the same for the diamond inclusions; 11. ilmenite: T°C [*Taylor et al.*, 1998]-P[kbar][*Ashchepkov et al.*, 2010]; 13. T°C and P [kbar] [*Brey and Kohler*, 1990]

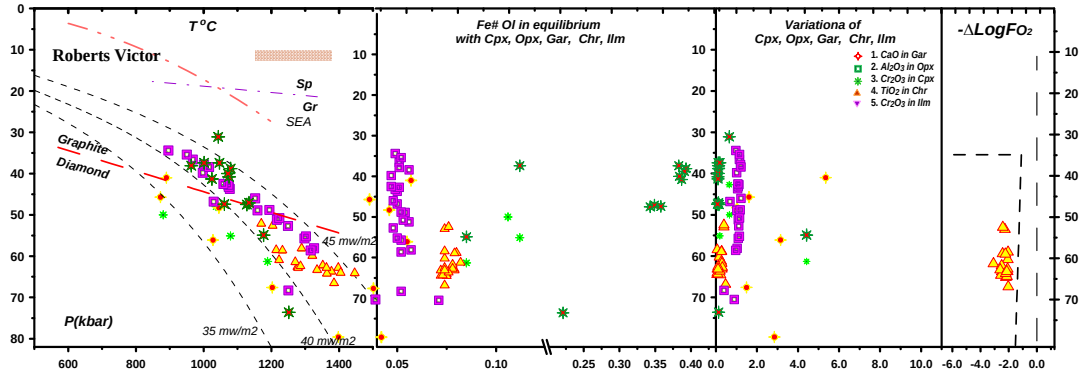

Fig 2. PTXF diagram for the SCLM beneath the Proterozoic Roberts Victor pipe S Africa. [*Hatton et al.,* 1979; *Jacob et al.,* 2005]

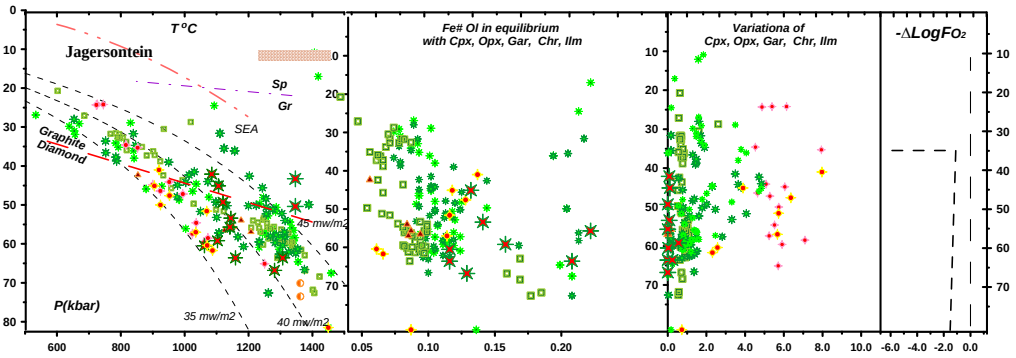

Fig 3. PTXF diagram for the SCLM beneath the Mesozoic Jagersfontein pipe S Africa [*Tappert et al.,*2005; *Tsai et al.*, 1979; *Winterburn et al.*, 1990]

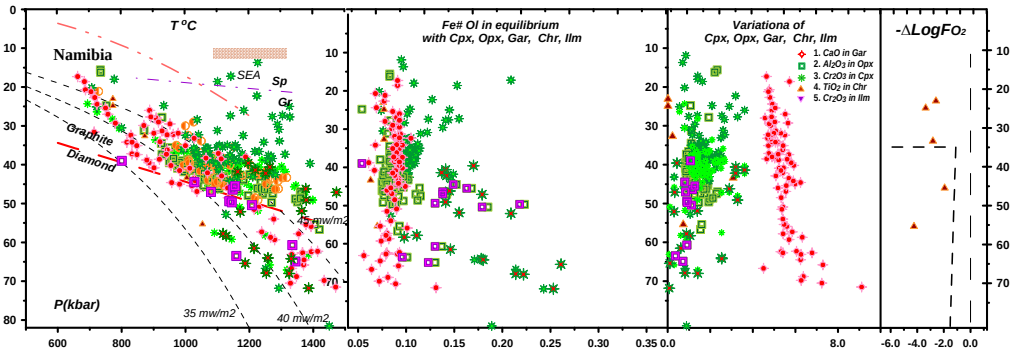

Fig 4. PTXF diagram for the SCLM beneath the Namibia [*Boyd et al.,*2005; *Harris et al.,* 2004.]

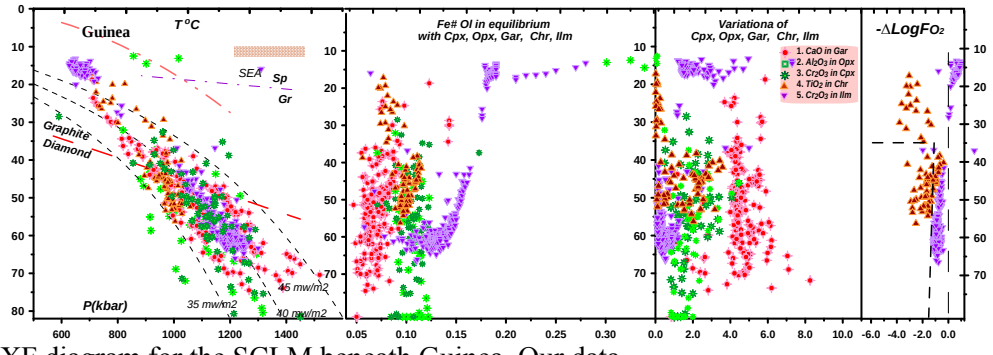

Fig 5. PTXF diagram for the SCLM beneath Guinea. Our data.

The off craton SCLM show the heated upper part of the mantle section like in Namibia [*Boyd et al.*, 2004] possibly created by the mantle diapirs. But SCLM in deeper part represented by diamond inclusions show similar hot and thick mantle 75 кбар [*Harris et al.,* 2004]. The SCLM in Congo Kasai

craton in Angola and Gunea show thicker and colder SCLM. But the rifted aria within craton show rather heated conditions like in Tansania, Labait volcano [*Aulbach et al.,* 2008] (Fig.5).

In North America the central part of the Slave craton show thick and relatively cold conditions like those found for Jericho and Panda pipe [*Cartigny et al.,* 2009]. But very often they like in Kaapvaal show double PT paths similar to those determined for SCLM beneath Lac de Gras [*Davies et al.,* 2004] (Fig 8). And younger pipes reveal heated conditions to 40 mw/m-2 like those beneath Torrie pipe [*MacKenzie, Canil,* 1999] (Fig.9). The SCLM beneath the Wyoming craton is rather thick and cool but in Mesozoic it is heated and probably reduced [*Hearn et al.,* 1999]

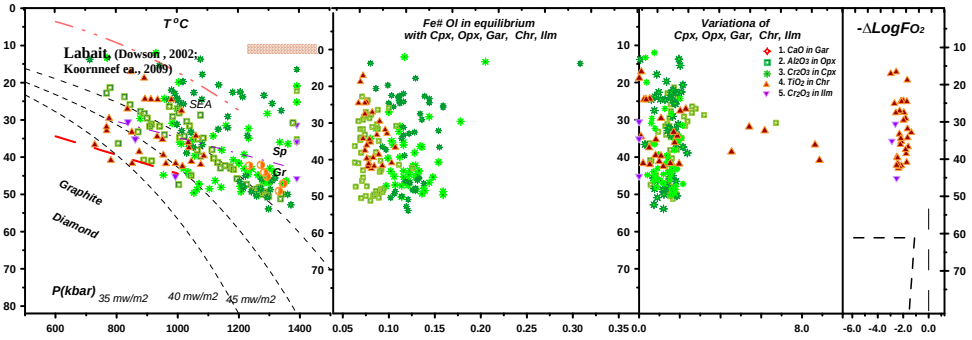

Fig. 6. PTXF diagram for the SCLM beneath Tansania rift [Aulbach et al., 2008].

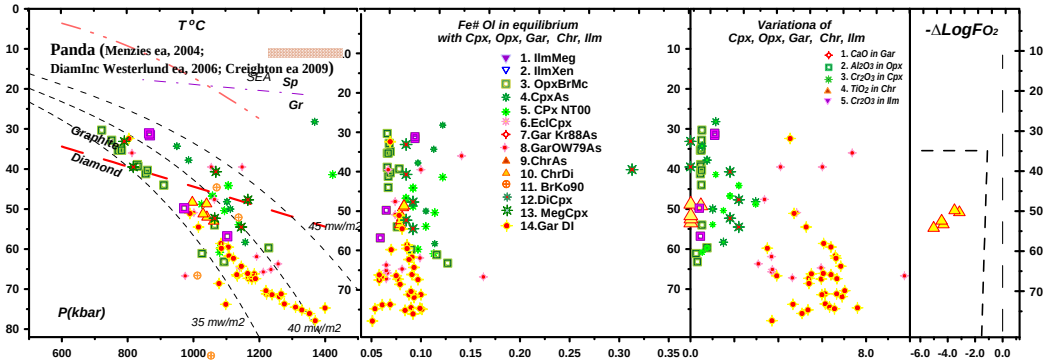

Fig. 7. PTXF diagram for the SCLM beneath Slave Craton [*Cartigny et al.,* 2009]

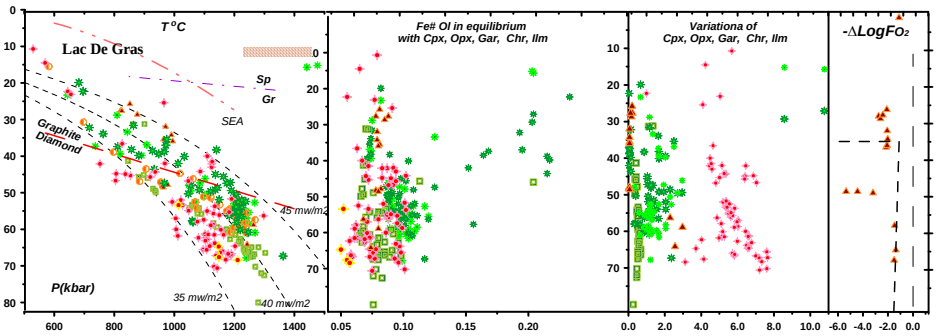

Fig. 8. PTXF diagram for the SCLM beneath Slave Craton [*Davies et al.*, 2004]

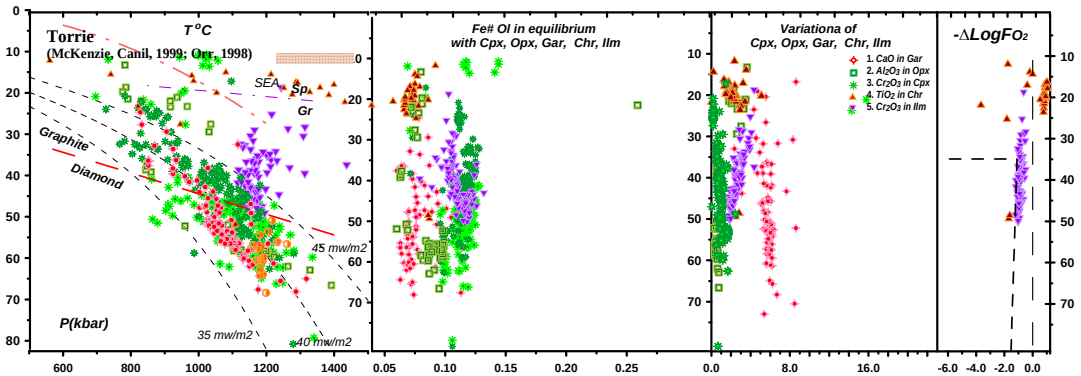

Fig. 9. PTXF diagram for the SCLM beneath Paleocene Torrie pipe [*MacKenzie, Canil,* 1999]

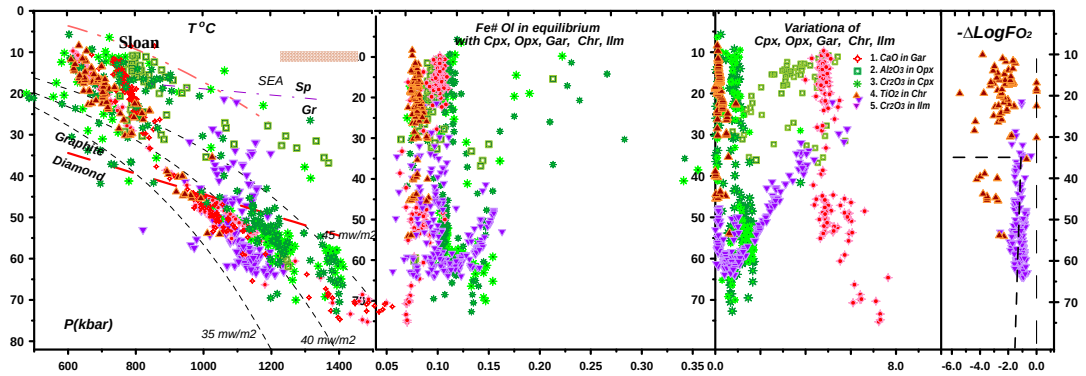

Fig. 10. PTXF diagram for the SCLM of the Paleozoic Sloan pipe Wyoming craton. Our data.

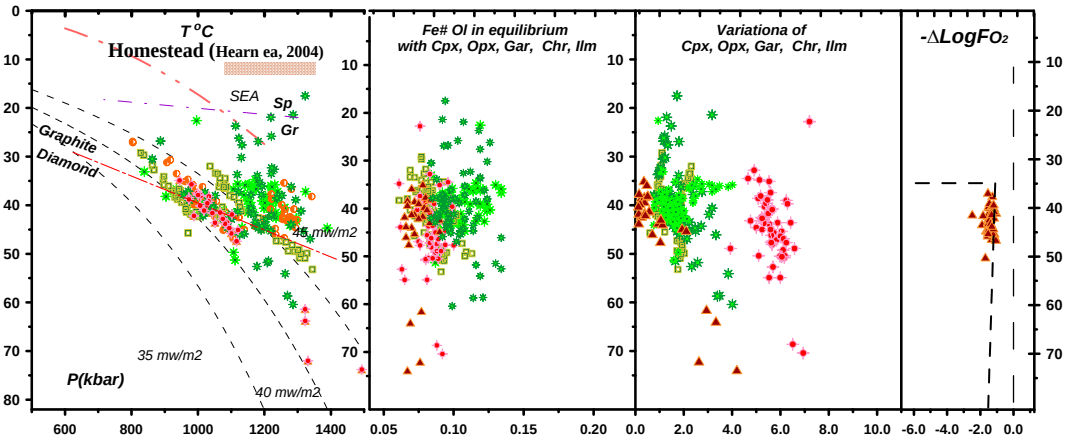

Fig.11. PTXF diagram for SCLM beneath Cretaceous Homestead pipe Wyoming craton. [*Hearn et al.*, 2004].

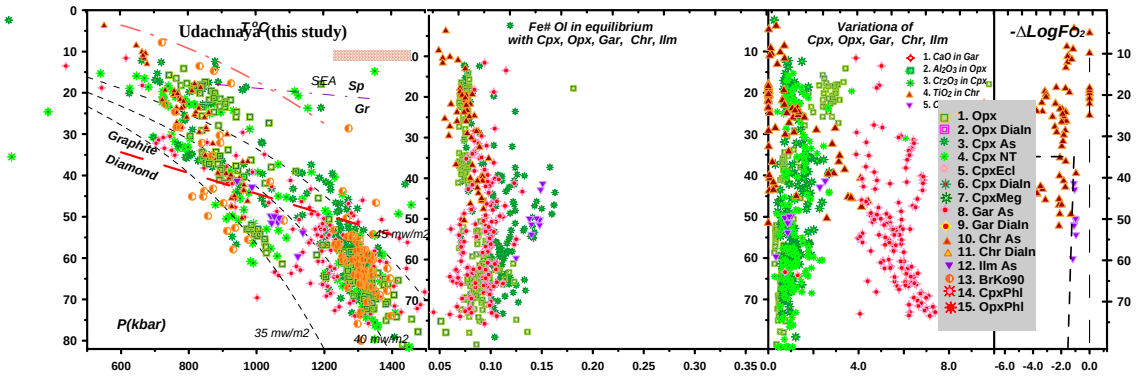

Fig.12. PTXF diagram fore SCLM beneath the Udachnaya pipe, Siberian craton. Our data

The layered structure of -7-12 horizons correlates with superplume events which is rather similar of the all ancient cratons. The more rough units commonly include 5-7 units like it was determined for Udachnaya pipe showing also deep and cold SCLM using new data set (Fig.12) [*Ashchepkov et al.,* 2010].

Models of the formation of the SCLM are : the nucleation of restite from early mantle it is diapiric, joining of ultra-exhausted blocks of Marianas and island-arc type thickened mantle blocks, the low angle subduction of partially melted plates under superplumes, breaking, cutting of high angle plates and joining to the continental margins. Slabs melting and diapir rising from the depths as deformed peridotites could also increase SCLM. Then fluid/melt flows in the continents margins modified mantle columns. Three traps for the melts: oxidized in- the SCLM base, carbonatite- 45-40 kbar, and water-bearing basaltic- 20-30 kbar were accompanied by the fusions and rising of diapiric at varying SCLM levels. This was accompanied by basification, lithosphere reductions and formation rifts in superplume periods.

Grants RBRF 11-05-00060a;11-05-91060-PICSa

References

Ashchepkov I.V., Pokhilenko N.P., Vladykin N.V., Logvinova A.M., Kostrovitsky S.I., Afanasiev V.P., Pokhilenko L.N., , Kuligin S.S., Malygina L.V., Alymova N.V., Khmelnikova O.S., Palessky S.V., Nikolaeva I.V., Karpenko M.A., Stagnitsky Y.B. (2010). Structure and evolution of the lithospheric mantle beneath Siberian craton, thermobarometric study. *Tectonophysics,* v.485, pp.17-41.

Aulbach S., Rudnick R. L. McDonough W. F. (2008). Li-Sr-Nd isotope signatures of the plume and cratonic lithospheric mantle beneath the margin of the rifted Tanzanian craton (Labait). *Contrib. Mineral. Petrol.* v.155, pp.79–92

Boyd F.R., Pearson D.G., Hoal K.O., Hoal B.G., Nixon P.H., Kingston M.J., Mertzman S.A.(2004) Garnet lherzolites from Louwrensia, Namibia: bulk composition and P/T relations. *Lithos* v.77, pp.473-491

Brey, G.P., Kohler, T. (1990). Geothermobarometry in four phase lherzolites II: new thermo-barometers and practical assessment of using thermobarometers. *Journal of Petrology* v.31, pp.1353-1378.

Cartigny P., Farquhar J., Thomassot E., Harris J. W., Wing B., Masterson A., McKeegan K., Stachel T. (2009). A mantle origin for Paleoarchean peridotitic diamonds from the Panda kimberlite, Slave Craton: Evidence from 13C-, 15N- and 33,34S-stable isotope systematics. *Lithos.* v.112 S2, 852-864.

Davies R.M., Griffin W.L, O'Reilly S.Y., Doyle B.J. (2004). Mineral inclusions and geochemical characteristics of microdiamonds from the DO27, A154, A21, A418, DO18, DD17 and Ranch Lake kimberlites at Lac de Gras, Slave Craton, Canada. *Lithos* v. 77, pp.39– 55.

Hatton, C.J., Gurney, J.J. (1979). Dimand graphite eclogite from the Roberts Victor Mine. In: F.R. Boyd and H.O.A. Meyer (Editors) *Proceedings of the 2nd International Kimberlite Conference, American Geophysical Union,* v. *2*, pp. 29-36.

Harris, J. W. Stachel, T., Léost, I., Brey G. P. (2004). Peridotitic diamonds from Namibia: constraints on the composition and evolution of their mantle source. *Lithos*, v.77, p. 209-223

Hearn C. (2004). The Homestead kimberlite, central Montana, USA: mineralogy, xenocrysts, and upper-mantle xenoliths. *Lithos.* v.77, pp. 473– 491

Jacob D. E., Bizimis, M, Salters, V. J. M. (2005). Lu–Hf and geochemical systematics of recycled ancient oceanic crust: evidence from Roberts Victor eclogites. *Contrib. Mineral. Petrol.* v.148, pp. 707–720.

McGregor, I.D. 1974. The system MgO–Al2O3–SiO2: solubility of Al2O3 in enstatite for spinel and garnet–spinel compositions. *American. Mineralogist* v.59 pp.110–19.

MacKenzie J.M., Canil D. (1999). CanilComposition and thermal evolution of cratonic mantle beneath the central Archean Slave Province, NWT, Canada. *Contrib. Mineral. Petrol.* v.134, pp.313 - 324

Nimis P., Taylor W. (2000). Single clinopyroxene thermobarometry for garnet peridotites. Part I. Calibration and testing of a Cr-in-Cpx barometer and an enstatite-in-Cpx thermometer. *Contrib. Mineral. Petrol.* v.139, pp.541-554.

O'Neill H.St.C, Wood B.J. (1979). An experimental study of Fe-Mg- partitioning between garnet and olivine and its calibration as a geothermometer. *Contrib. Mineral. Petrol.* v.70, pp.59-70

O'Neill, H. St. C. & Wall, V. J. (1987). The olivine orthopyroxene-spinel oxygen geobarometer, the nickel precipitation curve, and the oxygen fugacity of the Earth's upper mantle. *Journal of Petrology* v.28, pp. 1169-1191.

Richardson, S.H., Pöml P.F., Shirey S.B., Harris J.W. 2009. Age and origin of peridotitic diamonds from Venetia, Limpopo Belt, Kaapvaal–Zimbabwe craton. *Lithos,* v.112S, pp785–792

Simon N. S.C., Carlson R.W., Pearson D. G., Davies G. R. (2007). The Origin and Evolution of the Kaapvaal Cratonic Lithospheric Mantle. *Journal Petrology* v.48, pp.589 - 625.

Tappert, R., Stachel, T., Harris, J.W., Muehlenbachs, K., Ludwig, T., Brey, G.P. (2005). Diamonds from Jagersfontein (South Africa): messengers from the sublithospheric mantle, *Contrib. Mineral. Petrol.* v. 150, pp. 505–522.

Tsai, H.-M., Meyer, H.O.A. , Moreau, J., Milledge, J. 1979. Mineral inclusions in diamond :, Premier, Jagerfontein and Finsch kimberlites, South Africa, and Williams mine , Tansania. Proceedings of the 2nd International Kimberlite Conference, American Geophysical Union, v.2, pp.16-26.

Taylor W.R., Kammerman M., Hamilton R. (1998). New thermometer and oxygen fugacity sensor calibrations for ilmenite and chromium spinel-bearing peridotitic assemblages. 7th International Kimberlite Conference. Extended abstracts. Cape town. pp.891-901

Viljoen, K.S., Swash, P.M., Otter, M.L., Schulze, D.J. Lawless, P.J. (1992). Diamondiferous garnet harzburgites from the Finsch kimberlite, Northern Cape, South Africa. *Contrib. Mineral. Petrol.* v.110, p. 133-138

Winterburn, P.A, Harte,B., Gurney J.J., 1990. Peridotite xenoliths from the Jagersfontein kimberlite pipe: I. Primary and primary-metasomatic mineralogy. *Geochimica et Cosmochimica Acta*, v.54, pp.329-341